XMM's X-Ray Telescopes

D. de Chambure, R. Lainé, K. van Katwijk & P. Kletzkine
XMM Project, ESA Directorate for Scientific Programmes,
ESTEC, Noordwijk, The Netherlands

The XMM observatory has, at its heart, three large X-ray telescopes, which will provide a large collecting area (1430 cm^2 each at 1.5 keV, and 610 cm^2 each at 8.0 keV) with a spatial resolution of around 14-15 arcsec. At the end of 1998, three months ahead of schedule, the three flight and the two spare models of the X-ray telescope were handed over to the XMM Prime Contractor Daimler Chrysler Aerospace (D). The three flight models were integrated onto the spacecraft's optical platform at ESTEC at the end of March 1999.

The X-ray telescopes show mechanical and optical performances much better than specification, which will undoubtedly bring important benefits for astronomers. The most challenging parts of their development phase were the design, manufacture and testing of the X-ray mirrors, which required four intensive years of work under ESA's direct management (see ESA Bulletin No. 89, Feb. 1997).

This article focusses on the telescope design, with emphasis on the X-ray mirrors and baffles, and the X-ray and optical test results achieved with the flight models of the telescope, including stray-light reduction. Based on the lessons learnt from the XMM experience, the prospects for the next generation of ultra-thin X-ray mirrors are also addressed.

Introduction

The XMM spaceborne observatory has been designed as a high-throughput X-ray spectroscopy mission covering a broad band of energies, ranging from 0.1 to 12 keV. The heart of the payload consists of three telescopes (Fig. 1), developed under direct ESA contract by a consortium of several European firms, each with particular technical expertise for manufacturing specific parts of the telescopes.

The optics for each telescope consist of 58 nested Wolter-I grazing-incidence mirrors, or Mirror Modules, chosen to maximise the effective collecting area within the volume allocated. This highly nested design calls for the manufacture of a large number of X-ray-quality mirror shells. In 1993, after a competitive development programme, nickel electroforming technology was selected for the mirror production, with Media Lario (I) as Prime Contractor. Two years later, the yield ratio for the nickel mirrors was sufficient to successfully undertake the massive task of producing 311 X-ray-quality mirror shells – representing a total of 200 m^2 of high-quality optical surface – required for the start of the Qualification Model (QM) and Flight Model (FM) production phases. After the timely delivery of the QM Mirror Module, and after the completion of optical and environmental testing, the XMM Mirror Module was pronounced 'qualified' in October 1996.

By September 1998, the first four FM Mirror Modules had been delivered to ESA, and the acceptance and calibration tests were completed at Centre Spatial de Liège, the Max-Planck Institute and Dornier's facilities near Munich. At the end of 1998, three months ahead of schedule, the three selected flight models and the two spare models of the X-ray telescope were handed over to the XMM Prime Contractor, Daimler Chrysler Aerospace (Dornier). The three flight models were integrated onto the optical platform of the spacecraft in the clean tent in the ESTEC integration area at the end of March 1999.

The telescopes with the best optics have been chosen for flight, namely the FM2, FM3 and FM4 flight models. The two telescopes with the best resolution (FM3 and FM4) were allocated to the spectrometers (gratings + RGS detectors) and the EPIC MOS imaging camera, which have a better resolution than the EPIC p-n imaging camera. FM5 was not included in the selection since, being a spare, its delivery was foreseen after the date of selection and integration.

The X-ray baffle development, contracted to Sener (E), had to be completed in a short time, at a late stage in the XMM programme (after the start of the main development phase, C/D). Once the decision had been taken to reduce the X-ray stray light by including an X-ray baffle, it took the XMM Project only seven months to design it, to demonstrate manufacturing feasibility, and to verify that the telescope's performance was not degraded in terms of resolution, effective area and optical stray light.

Telescope design

The three telescopes consist of the following elements (Fig. 2):

- mirror assembly door: closes and protects the X-ray optics and the telescope's interior against contamination during integration, testing, transport, launch and the early orbit phase
- entrance baffle: provides the stray-light suppression capability in the visible wavelength range at angles larger than 47°. It consists of a cylindrical aluminium shell with an outer diameter of 870 mm. The inside is covered by 12 circumferential vanes and is optically black. Due to volume constraints under the Ariane-5 launcher fairing, the baffle length is limited to 900 mm, including the protrusion of 200 mm below the separation plane into the launch adapter. They are mounted after the integration of the Mirror Modules on the spacecraft
- X-ray baffle (XRB): blocks X-rays from just outside the nominal field of view, which would otherwise reflect on the hyperboloid section of the mirrors, resulting in stray light
- Mirror Module (MM): the X-ray optics of the telescope
- 'electron deflector' (produces a toroidal magnetic field): located right behind the mirrors (in the shadow of the Mirror Module spider), for diverting 'soft' electrons (with energy up to 100 keV)

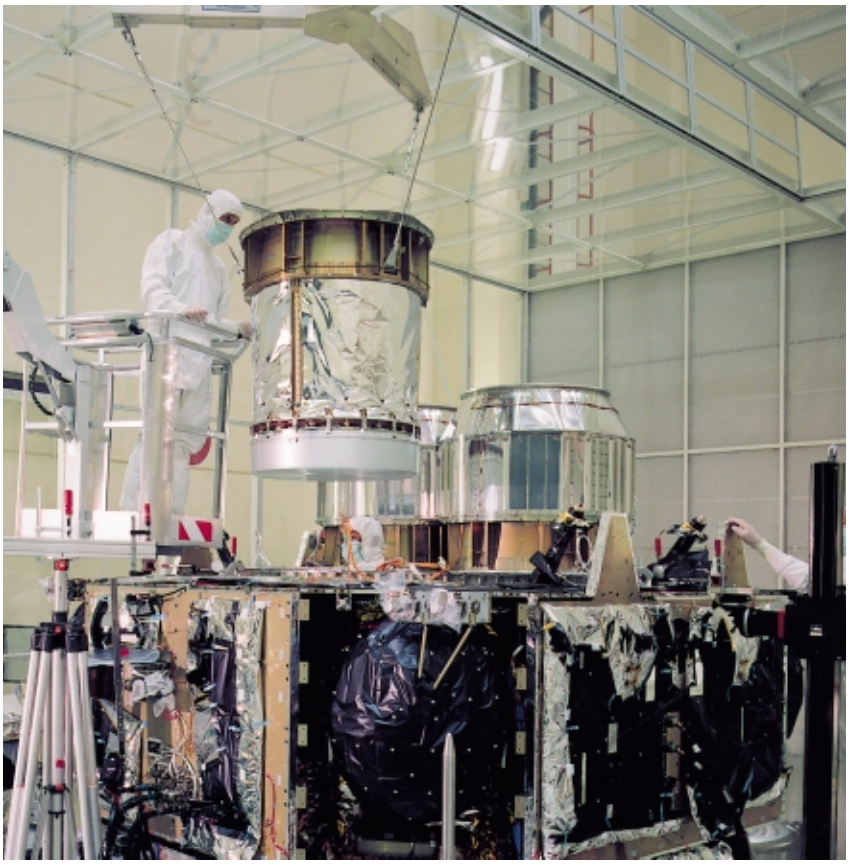

Figure 1. Integration of the three X-ray telescopes on the XMM spacecraft inside the class-100 area of the ESTEC Test Centre (Noordwijk, NL)

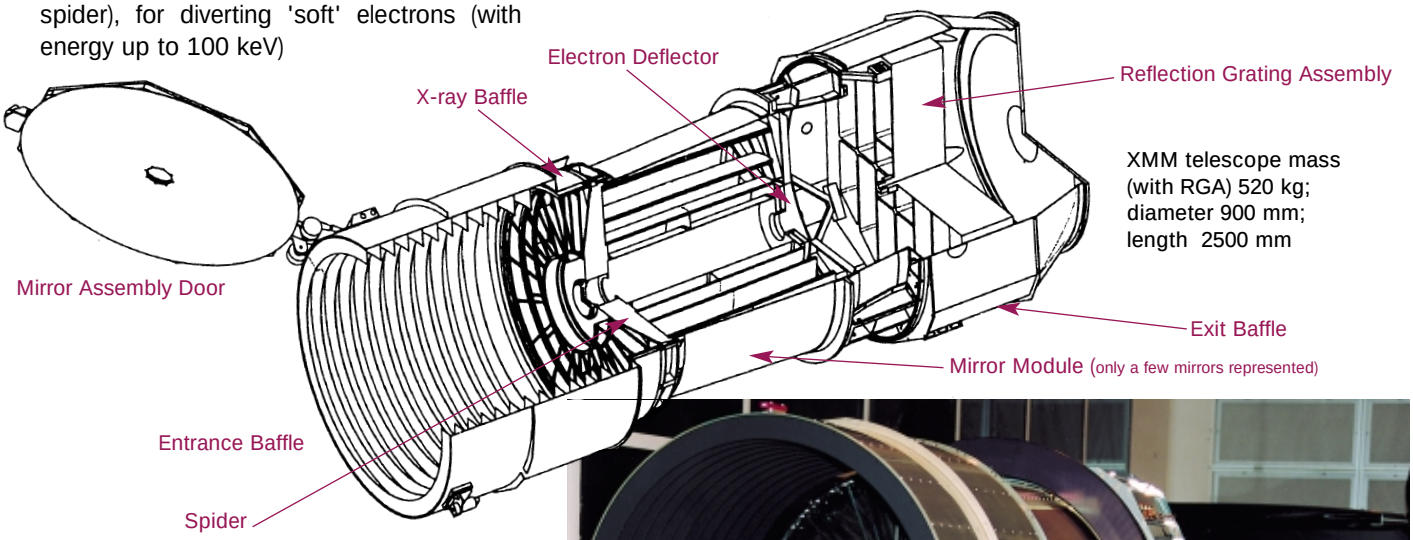

- Reflection Grating Assembly (RGA): has a mass of 60 kg, on the backside of two out of three Mirror Modules, corresponding to the telescopes 1 and 2. It deflects roughly half of the X-ray light to a strip of CCD detectors (RGS), offset from the focal plane and includes 182 reflection grating plates (100 x 200 mm), mounted and aligned in a beryllium-alloy structure. Each grating plate is replicated from a master, onto a silicon-carbide substrate
- exit baffle: provides a benign thermal plate environment for the gratings and the Mirror Module.

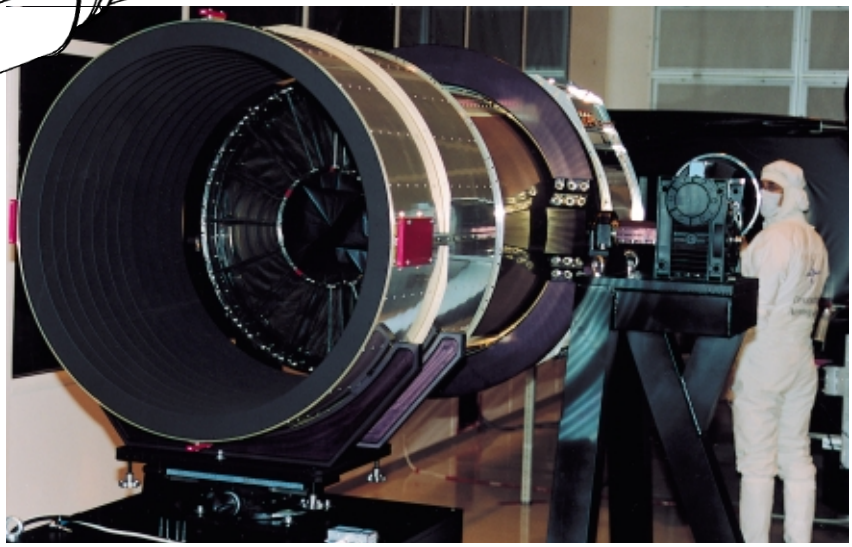

Figure 2. Design and view of XMM telescope during wide-angle stray-light testing at Dornier (Ottobrunn, D)

Mirror Module

A Mirror Module is a grazing-incidence telescope (Wolter-I type) which is designed to operate in the X-ray energy range of 0.1-12 keV with a focal length of 7.5 m and with a resolution of 16 arcsec. A Mirror Module consists of 58 nested mirror shells bonded at one end to a spider (or spoked wheel) and their supporting structure. The grazing angle of the X-rays ranges from 17 arcmin for the smallest mirror to 40 arcmin for the largest. The optical concept of the XMM Mirror Module is shown in Figure 3.

Figure 3. Optical design of the XMM Mirror Module with the EPIC and RGS detectors

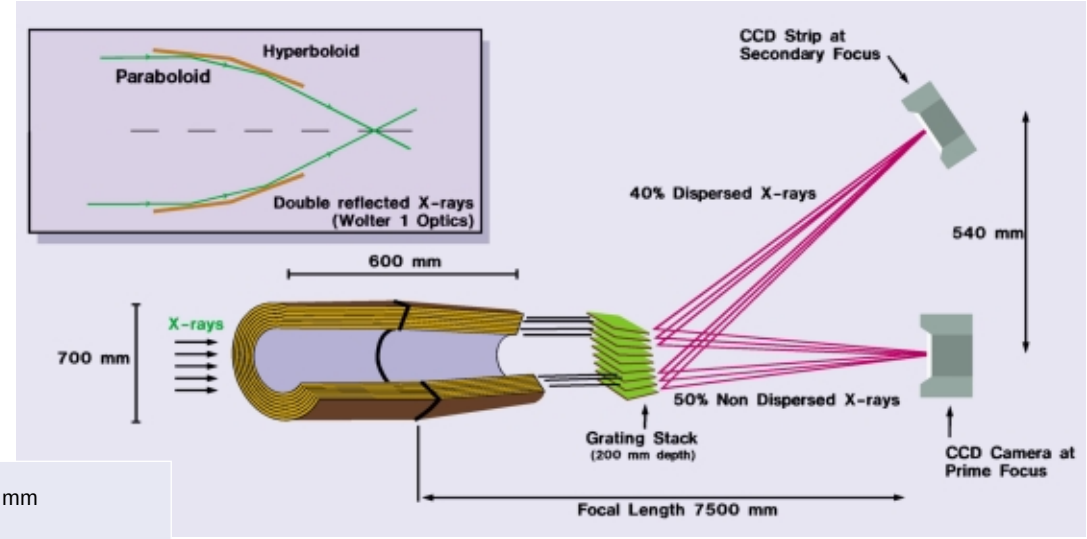

Focal length	7500 mm
Resolution	
Half Energy Width	16 arcsec (0.1-12 keV)
Full Width Half Max	8 arcsec (0.1-12 keV)
Effective area	
	1475 cm^2 (1.5 keV)
	580 cm^2 (8 keV)
	130 cm^2 (12 keV)
Mirror diameter and thickness	
Outermost	700 mm (1.07 mm)
Innermost	306 mm (0.47 mm)
Mirror length	600 mm
Packing distance	1- 5 mm
Number of mirrors	58
Reflective surface	Gold (250 nm layer)
Mirror Module mass	420 kg

The mechanical design of the Mirror Module is shown in Figure 4. Each mirror is shaped to a paraboloid surface in front and a hyperboloid surface at the rear for double reflection of the grazing X-rays. The 58 mirror shells are mounted in a confocal and coaxial configuration. The shells are glued at their entrance plane to the 16 spokes of a spider (spoke wheel) made out of Inconel. This material was chosen for its thermal expansion, which is close to that of the electrolytic nickel of the mirrors. The spider is connected to the platform of the XMM spacecraft via an aluminium interface structure, the Mirror Interface Structure (MIS), which consists of a double conical surface reinforced by stiffeners and an interface ring. To minimise the mechanical deformations of the mirrors and therefore the optical degradation, the flatness of the mounting interface between the spider and the MIS, which is a surface with an inner diameter of 740 mm and an outer diameter of 770 mm, needs to be better than 5 µm. Heaters and thermistors, mounted on the spokes and the outer ring of the spider, provide the thermal control for the Mirror Module at 20ºC ± 2ºC, with transverse and radial gradients not exceeding 2ºC.

The X-ray mirrors are thin monolithic gold-coated nickel shells. The mirror shell manufacturing is based on a replication process (Fig. 5), which transfers a gold layer deposited on the highly-polished master mandrel to the electrolytic nickel shell, which is electroformed on the gold layer. The production of the required 58 master mandrels was contracted to Zeiss (D). They are initially made out of double conical aluminium blocks coated with Kanigen nickel, then lapped to the exact shape and, finally, super-polished to a surface roughness better than 4 Å (0.4 nm).

Due to the sensitivity of the mirrors in the way they are supported, the most critical steps in the manufacturing of the Mirror Module are the

Figure 4. Mirror Module mechanical design

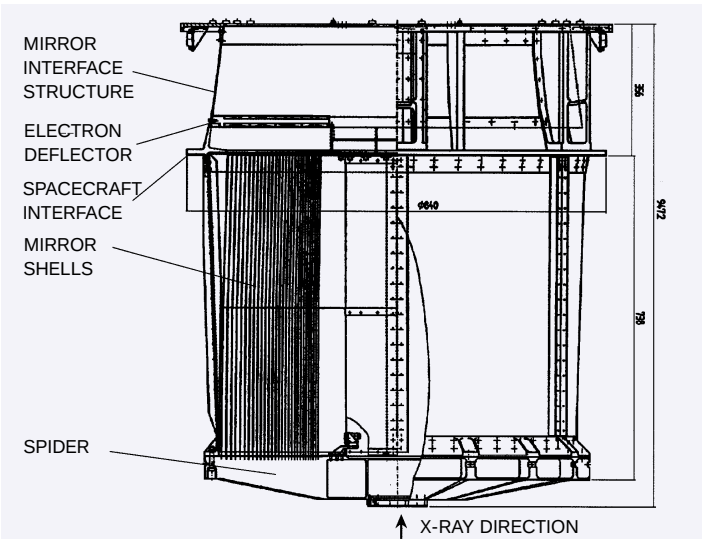

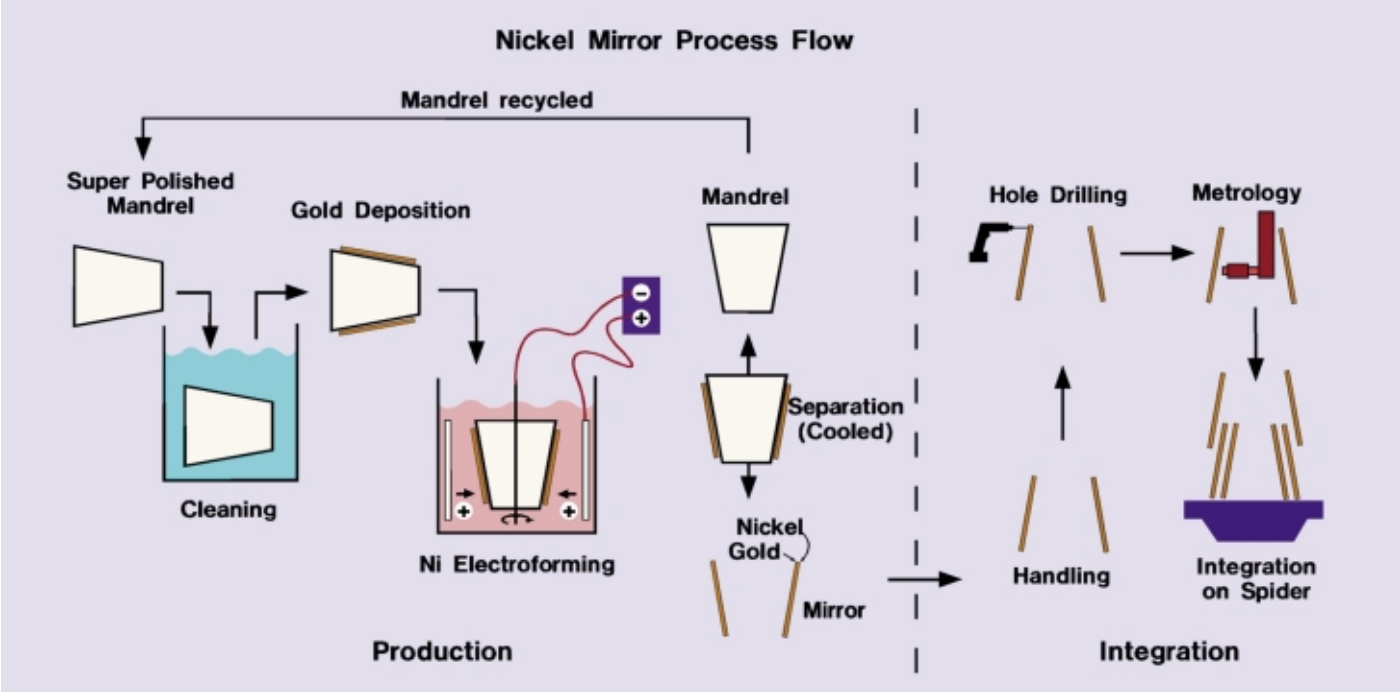

Figure 5. Mirror production and integration process

production of the mirror shells and their integration onto the spider. Indeed, the XMM mirrors are very fragile, their diameter-to-thickness ratio being in the order of 324, ten times as large as for SAX or JET X telescopes.

The technological development and the management of the XMM X-ray mirror programme have been detailed in a previous issue of the ESA Bulletin (No. 89, February 1997).

X-ray baffle

Single reflections from one or more of the hyperboloid surfaces introduce a high level of confusing stray flux in the Field of View (FOV) of the detectors. This occurs for objects located close to, but outside, the FOV (cone angle of 15 arcmin). Previous X-ray telescopes with a small number of mirrors could be protected from such effects by individual shells in front of each mirror. However, highly nested telescopes, such as ASCA, are not baffled due to the limited space between the mirrors. This represents an important limitation for ASCA that produces significant stray light and complicates the evaluation of the observation data. This stray light can only be suppressed by using a 'pre-collimator' (or X-ray baffle) consisting of thin cylindrical shells, which extend the mirror shells forward. In order to reduce reflection and scattering from the cylindrical surfaces, cylindrical sections can be removed leaving thin circular annular rings (strips) in front of each mirror (Fig. 6).

Figure 6. Principle and 3D view of the X-ray baffle

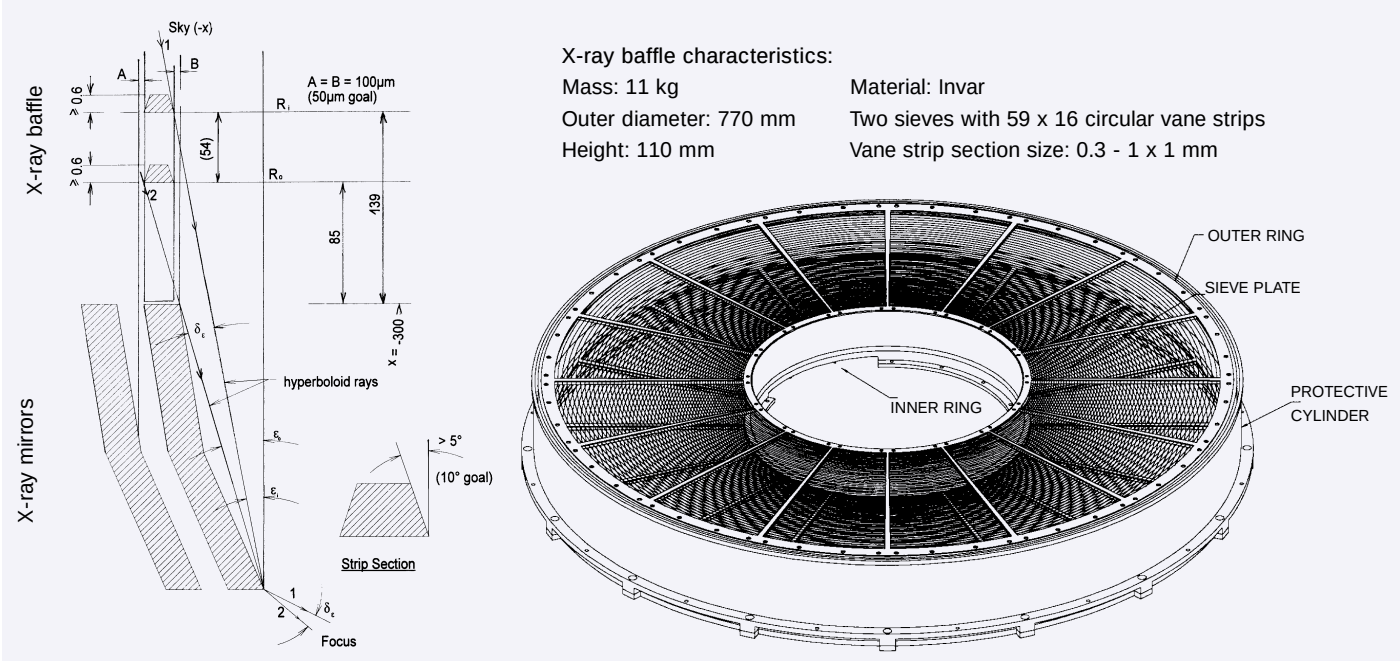

Thus, the X-ray baffle is constructed as a series of 'sieve plates', made out of circular strips. These plates are mounted in line with the front face of the mirrors, such that they block single-reflection rays, but do not eclipse the bona fide two-reflection rays. In the XMM telescope, the axial space available allows for two such plates to be incorporated into the X-ray baffle. This blocks about 80% of the single-reflection flux.

Each sieve plate is basically a disc, with 59 circular strips and 16 radial spokes, and therefore 59 x 16 slots. The thickness of the disc is 1 mm, except for the stiffeners located on the spokes and the outer annular ring, where the thickness is locally 5 mm. In order to reduce the optical stray light, introduced by the X-ray baffle, to a maximum extent, the lateral surfaces of the strips are chamfered by 5º and the edges of the strips are made very sharp (radius smaller than 20 µm). All the baffle surfaces (including the edges of the vane strips) facing the mirrors are blackened.

The main requirement placed on the X-ray baffle is the accuracy of the radial position of the edges of the vane strips of the sieves with respect to the position of the mirrors. It must be better than 100 µm, including manufacturing, assembly and integration errors, and displacement due to thermal conditions (-10ºC to +10ºC).

The fulfilment of this high tolerance requirement relies on:
- the selection of a high-quality Invar material, with a very low coefficient of thermal expansion ($< 10^{-6}\ ^{\circ}C^{-1}$), for the sieve plates and their support structure (inner and outer ring)
- the accurate machining of each sieve plate
- the accurate positioning of both sieve plates on their support structure and, subsequently, of the X-ray baffle on top of the Mirror Module, with the help of a 3D measuring machine.

The main challenge in the manufacturing of the baffle was the machining of the large and flexible Invar sieve plate, with its 59 x 16 'tiny' strips, with a precision better than 65 µm. After having analysed several potential machining processes (among them photochemical etching and laser cutting), Wire Electrical Discharge (WED) machining proved to be the most adequate, although it has the disadvantage of involving long machining times. Each sieve plate needed between 400 and 500 machining hours, which led to the use of two WED machines in parallel. The verification of each sieve plate was performed on a 3D-measuring machine. The radial position of the edges with respect to the centre of the sieve plate was measured at 10 points per slot, i.e. 9280 points per sieve plate. The results obtained with the chosen WED machining procedure were good, with a mean value for the radial errors of about 25 µm and a standard deviation of about 35 µm.

Optical and environmental testing of the telescopes

Acceptance test programme for the Mirror Modules

It was realised early on that a large amount of X-ray telescope testing had to be performed. The 'Panter' X-ray facility of the Max-Planck Institute (MPE) at Neuried, Germany was available to XMM. However, several aspects pleaded for the creation of a new test facility. In addition to the sheer amount of testing of the telescopes, the Panter facility was to be used for tests on XMM's scientific cameras. The fact that the telescopes tested at Panter had to be in the horizontal position was not insignificant for such thin mirror shells, and parasitic gravity effects could not be excluded. Most importantly, for the measurement of the optical performance, a third of the mirror shell surface could not physically be properly illuminated because of the slight divergence of the X-ray beam. The ESA XMM Project office therefore decided, in 1994, to complement the Panter facility by building a custom-designed, vertical facility equipped with an 800-mm EUV collimator and two thin X-ray beams, adapted to the dimensions of the telescopes. This facility, called 'Focal-X', is located at Centre Spatial de Liège (CSL) in Belgium. Two aspects motivated the choice of EUV light (at 58 nm):
- the negligible level of diffraction effect
- the possibility of using fairly standard off-the-shelf technologies for the optical components, especially the detectors.

The choice of Centre Spatial de Liège was logical due to:
- its world-famous experience in the testing of optical systems for space applications
- its qualification as an ESA coordinated facility
- the on-site availability of vibration and thermal-vacuum facilities, limiting handling and transport of the telescopes.

Starting in February 1997, after their staggered delivery to ESA, the five Flight Models of the XMM Mirror Module (Fig. 7) were optically, mechanically and thermally tested at the Panter X-ray facility, the Focal-X facility, and the CSL test centre. The acceptance programme included, in chronological order, the following tests:

– extreme ultraviolet (EUV) optical and X-ray reflectivity tests at the Focal-X facility
– vibration tests followed by thermal-vacuum testing at CSL
– EUV optical and X-ray reflectivity tests at the Focal-X facility
– X-ray optical tests at the Panter X-ray facility.

The purpose of these tests was to demonstrate that the FM Mirror Modules fulfilled the performance requirements after exposure to simulated environmental conditions at least as severe as those expected during the service life of the XMM spacecraft. In order to verify their structural integrity, the FM Mirror Modules were subjected to vibration tests simulating the Ariane-5 launch environment and to thermal-vacuum tests representing the in-orbit conditions. The vibration tests were performed on the shaker at CSL. The Mirror Modules were subjected to sinusoidal and random vibration along the X, Y and Z-axes at acceptance level (10 g axial and 6.7 g lateral). The thermal tests (3 cycles between –20ºC and 40ºC) were performed in the Focal-2 thermal-vacuum test chamber at CSL.

The environmental tests on the FM Mirror Modules were successful because the following criteria were fulfilled:
– the specified test input loads were applied
– the fundamental frequencies were within specification and did not vary significantly after the high-level vibration tests
– no visual damage was observed after the environmental tests
– the optical performance had not deteriorated due to the vibration and the thermal tests (see below).

Calibration test programme for the telescopes

Following the acceptance testing on the Mirror Modules, calibration tests were performed on the complete telescopes, with or without the Reflection Grating Assembly (RGA), depending on their final position on the spacecraft. The purpose of these tests was to:
– assess the optical performance of the X-ray baffle (vignetting, stray-light rejection, etc.)
– characterise the performance of the RGA (line profile at selected energies; effective area as a function of energy; resolving power, positions of 0,1st and 2nd order focii, etc.)
– determine the level of stray light in the EUV, visible and near-infrared going through the telescope
– validate the software model of the telescope.

The choice of the combination of the optics, the gratings and the detectors was dictated by the scientific objectives of the XMM mission. In view of the lower resolution of the EPIC p-n detector (pixel size 140 µm) compared to the RGS and the EPIC MOS detectors (pixel sizes 27 and 40 µm), the two Mirror Modules with the best resolution were combined with the RGS and EPIC MOS instruments. Therefore, these two Mirror Modules (currently FM3 and FM4) are equipped with the RGAs.

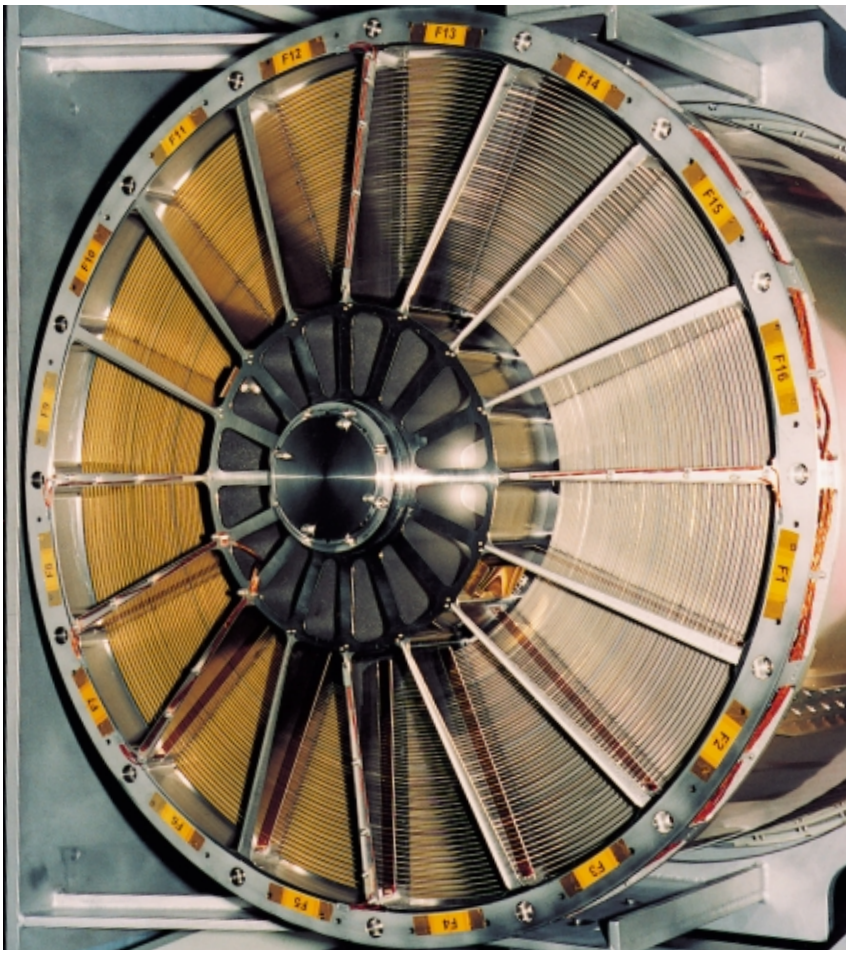

Figure 7. Mirror Module entrance plane with the 58 X-ray mirrors

The performance of the X-ray baffle is mainly assessed by measuring the effective area at various off-axis angles in two orthogonal directions and by checking the relative positioning of the mirrors with respect to the strips with the pencil beam (see below).

The precision alignment and assembly of the grating elements of the RGA were performed at Columbia Astrophysics/Nevis Laboratory, and the end-to-end calibration and testing were performed at the Panter and Focal-X facilities. These tests confirmed that the effective area for both RGS spectrometers is approximately 150 cm^2 at 0.15 nm. The measured resolving power of RGA2 has exceeded predictions because of the high performance of the Mirror Modules, while it falls short slightly for RGA1 due to grating-array fanning misalignment introducing an aberration that is not completely correctable.

Stray-light tests were performed in the EUV, visible and near-infrared spectral ranges, in order to verify the predictions obtained from the stray-light calculations. These tests were carried out at small angles, up to 7.5º, with the Mirror Module plus X-ray baffle and at large angles, from 10º up to at least 47º, with the complete telescope. At small angles, the entrance baffle was not tested because it is not a stray-light contributor (not illuminated by the Earth). Other spacecraft components (i.e. telescope Sun shield; telescope tube) were not present in the stray-light tests due to their large dimensions. Also, they are not considered as important verification subjects, since optical analysis has shown that the corresponding stray paths lead to negligible stray-light levels.

Small-angle stray-light tests were performed at the Focal-X facility. They acquired images for sources located between 20 arcmin and 7º in the visible and in the EUV. This was achieved by tilting the optical bench (supporting the tested telescope), the tower and the upper optical focal bench with the detectors (made as a single structure) and by translating the CCD at different locations to completely cover the EPIC or the RGS Field of View (FoV). Indeed, the CCD is 18 mm x 25 mm, the EPIC FoV has a diameter of 66 mm, and the RGS FoV is rectangular and 25 mm x 250 mm. The images were then analysed and compared to simulations performed with a ray-tracing programme. For all off-axis angles at all azimuthal positions, the test results confirmed the simulations, both qualitatively in terms of image quality and quantitatively in terms of integrated collecting area in the EPIC and RGS FoV.

Large-angle stray-light tests were performed in the large clean room (class 100) at Dornier in August 1998. The test set-up included the light source with a xenon arc lamp, the collimator, the telescope to be tested and a light trap in the direction of the telescope FoV. The test detector was moved to the position of the EPIC and of the RGS camera, where the Point Source Transmittance (PST) was measured and compared with the analysis results. The PST is defined as the integrated stray-light irradiance at the detector divided by the source irradiance at the entrance of the telescope. The measurement of the signal-to-noise ratio (S/N) has shown that the complete optical chain with the source, the optics, the telescope and the chosen CCD test detector is not noise-limited. In fact, it is limited by the scattering of the air and particles, and by the backscattering from the walls of the test facilities within the direct FoV of the telescope. Both are responsible for a background PST in the order of 10^{-9}. Therefore, the stray-light calculations were verified for a large range of angles of incidence of the incoming radiation, except for angles close to 70 - 90º, where the residual PST in the test configuration was too high.

EUV and X-ray results at Centre Spatial de Liège (CSL)

Image quality and effective area in the EUV

The image quality (Full Width Half Maximum (FWHM), Half Energy Width (HEW), 90% Encircled Energy (W90)) of the five Flight Models of the Mirror Module, measured in EUV (58 nm) at CSL, is summarised in Table 1. The EUV tests showed no significant differences in the Encircled Energy Function (EEF) before and

Table 1. Image quality of the Flight Model Mirror Modules from CCD measurements at CSL before (pre-env) and after (post-env) environmental tests compared to the Qualification Model of the Mirror Module at 58 nm

Mirror Module model	MM QM	MM	FM1	MM	FM2	MM	FM3	MM	FM4	MM	FM5
Position on S/C	N/A	Flight	spare	No	RGA	with	RGA2	with	RGA1	Flight	spare
Optical test (58 nm)	Post-env	Pre-env	Post-env	Pre-env	Post-env	Pre-env	Post-env	Pre-env	Post-env	Pre-env	Post-env
HEW at best focus (arcsec)	19.5	15.8	15.5	16.1	15.4	14.2	14.0	13.7	13.9	11.7	11.7
FWHM at best focus (arcsec)	10.2	6.7	6.7	6.9	6.3	5.5	4.5	4.9	4.9	4.9	4.9
W90 at best focus (arcsec)	110	62	63	63.5	62	58	59	62	63	53	55
Focal length (mm)	7496.0	7493.0	7493.0	7493.2	7493.2	7493.7	7493.6	7493.4	7493.4	7494.7	7494.7

Table 2. Measurements of X-ray reflectivity (in %) of mirror sizes 1, 20 & 58 (incidence angles respectively 40, 30 & 17 arcmin) of the 3 telescopes to be flown

Model	FM2			FM3			FM4			Theory (Henke 93)		
Mirror size	1	20	58	1	20	58	1	20	58	1	20	58
Reflectivity at 1.5 keV	68	75	87	69	76	85	63	74	83	76	81	89
Reflectivity at 8 keV	0.5	38	74	0.3	39	73	0.3	37	69	<0.5	43	78

after environmental tests. The overall performance in terms of resolution indicates an important improvement compared to the QM Mirror Module:

– the core of the Point Spread Function (PSF) is very sharp (no double peak as for the QM Mirror Module), especially for Mirror Modules FM3 and FM4 with a FWHM of 4.5 arcsec (Fig. 8)
– the resolution (HEW) is better than for the QM Mirror Module (measured at 20 arcsec) and has been continuously improved
– the W90 has been improved compared to the QM Mirror Module, which was at 100 arcsec, due to reduced deformation of the edges of the mirrors.

The focal images of Mirror Modules FM1 and FM2 (Fig. 8) show a 'triangular' shape, which comes from the distortion of the outer mirror shells (see below). This distortion, responsible for a performance loss estimated to be in the order of 1-2 arcsec for FM1 and 2 arcsec for FM2, occurred during the integration of the Mirror Module. Indeed, several analyses have confirmed that the deformation of the outer mirrors is the result of the unevenness between the spider and the Mirror Interface Structure (flatness of 15 - 25 µm instead of the specified 5 µm), aggravated by small deformations of the integration adapter, on which the spider was mounted during the integration of the mirrors. This point was not identified for the QM Mirror Module as no large X-ray-quality mirror could be integrated in that model. A shimming method was developed and tested, which has been successfully implemented on FM3 and, to a lesser extent, on FM4 and FM5.

X-ray reflectivity tests

The X-ray reflectivity (double reflection) of the five Flight Models of the Mirror Module was measured at several energy levels. Reflectivity measurements were performed in the middle of the mirrors along two azimuths with a pencil beam (diameter 0.5 mm at the entrance of the mirrors with a maximum divergence of 8 arcsec half angle). For each mirror, the reflectivity is the ratio of the integrated counts in the area of interest of the reflected and the incident beam, on a germanium solid-state detector, closed by a beryllium window. The measurement accuracy of the method is estimated to be ± 1-2%. In Table 2, the X-ray reflectivity values have been indicated at 1.5 and 8 keV, for some representative mirrors (largest size #1; smallest size #58 and one with an incidence angle close to critical angle, size #20) of the 3 telescopes to

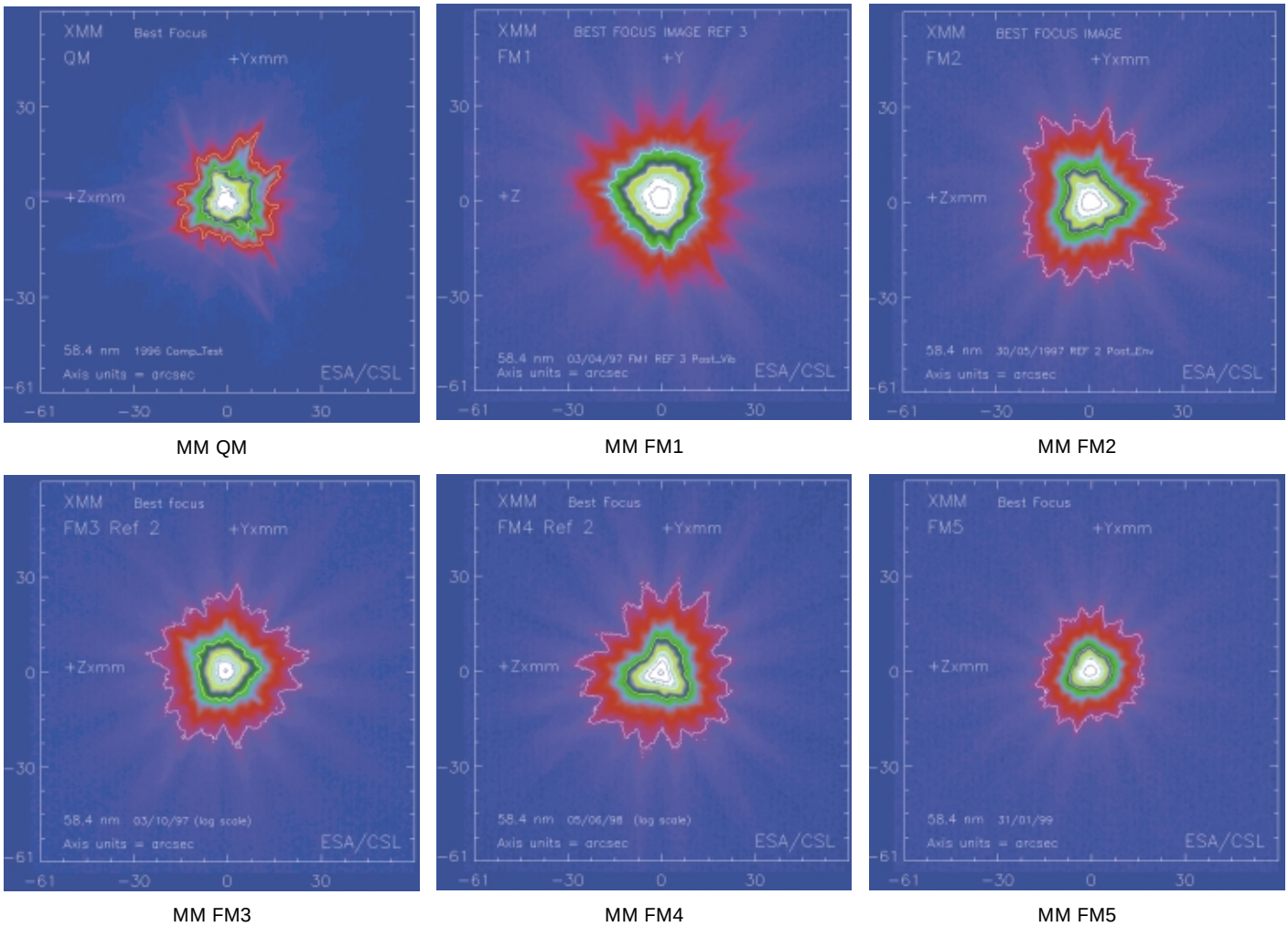

MM QM | MM FM1 | MM FM2

MM FM3 | MM FM4 | MM FM5

Figure 8. Point Spread Function of the QM and FM Mirror Modules (log scale of intensity)

be flown. It shows that the reflectivity of the mirror is good, representing a loss per reflection of only 2 - 3% at 1.5 keV and 3 - 4% at 8 keV. The values take into account corrections for the loss of reflectivity due to scattering of the incident beam outside the detector field (detector diameter 20 mm): 0.6% at 1.5 keV and 6% at 8 keV.

At all energy levels, there was no degradation after each optical/environmental test: values were stable within the measurement accuracy with the exception of the shells (sizes #54, #49 and #45) with high fluctuations (about 10 - 20%). These mirrors are known to have a locally poor micro-roughness (around 0.8 nm measured with Promap interferometer), due to some mandrel surface degradation after a certain number of replications.

X-ray test results at Max-Planck Institute (MPE)

The image-quality figures (Full Width Half Maximum (FWHM), Half Energy (HEW), 90% Encircled Energy (W90)) of the five FMs of the Mirror Module measured at the Panter facility in the period April 1997–July 1999, are summarised in Table 3 and in Figure 9. The Mirror Modules were tested in full illumination (horizontal X-ray beam with a source at 124 m) at different X-ray levels between 0.1 keV and 10 keV, with two different detectors: a Position-Sensitive Proportional Counter (PSPC) and a Charge-Coupled Device (CCD). The PSPC has a diameter of 76 mm, equivalent to a diameter of 980 arcsec in the focal plane, whereas the CCD has a size of 20 mm x 13 mm, which does not cover the wings of the PSF completely. Therefore, reliable W90 measurements could only be obtained with the PSPC.

The X-ray results of the HEW and FWHM measurements give values almost identical to those obtained at CSL, within the measurement accuracy of the facility, which was not the case for the QM Mirror Module. This confirms that the improvements made to the mirror geometry, especially at the edges (affecting 10% of the mirror surface), which are not 'seen' at Panter due to its finite source distance, were successful.

Performances at X-ray energy levels higher than 6.4 keV were slightly better than at 1.5 keV because of the small contribution of the large size mirror shells (effect amplified by the finite source distance) and because of the better quality of the inner mirror shells. In Figure 9, the triangular shape of the core of the focal image is no longer visible at high energy levels (above 4.5 keV), clearly confirming that the triangularisation is coming from the large outer mirrors. The shadowing structures are entirely due to the spider spokes. The images in Figure 9 and the data in Table 3 clearly show that the power in the wings increases at energies between 0.9 keV and 6.4 keV, while the central part does not change significantly. For the higher energy levels, the core and the wings get smaller, since the outer mirrors are no longer contributing, due to the finite source distance and the lower reflectivity of the large mirrors. In conclusion, the mirror scattering, which is expressed in the W90 at high energies, is much better for FM Mirror Modules than for the QM Mirror Module, which was measured at about 240 arcsec at 8 keV.

The determination of the effective area was based on a relative measurement. The same detector (PSPC) was used to measure the count rate of the flux with and without the Mirror Module in the beam. This method has the advantage that most of the properties of the detector do not need to be taken into account for the computation of the effective area. The measurements were done at full illumination with the PSPC moving slightly laterally (few mm) in intra-focal position (100 mm) to avoid obstruction by the wire mesh that supports the detector entrance window. The method's precision was better than ±2%.

For all the FM Mirror Modules, the effective areas measured with full-aperture illumination were systematically 15% lower (both at 1.5 keV and 8.0 keV) than the 'theoretically' achievable value. The results of these full illumination tests have been difficult to analyse because of secondary shadowing due to the geometry of the Panter facility (finite source distance) with respect to the tight nesting of the mirrors. Complementary tests with a reduced beam aperture gave a more reliable estimate of the effective area, with a loss of less than 10% compared to theory. The area is very close to the specified value, as shown in Table 4. The deficit observed in the quasi-parallel beam test was partly due to the reflectivity of the mirrors (see section 'X-ray refectivity tests'), but also to some over-thickness of the mirrors at their edges (protruding burrs from the electroforming process).

X-ray baffle tests at Centre Spatial de Liège (CSL) (Fig.10)

To check the correct positioning of the X-ray baffle on the spider of the Mirror Modules, several optical tests were carried out to ensure that the on-axis optical performance of the telescope remained unchanged after the mounting of the baffle, i.e. no on-axis vignetting effect and no image-quality degradation.

Table 3. X-ray image quality of the five Flight Models of the Mirror Module at best focus, in arcsec (HEW data corrected by quadratic subtraction of the intrinsic resolution of the PSPC at the corresponding energy)

	FM1			FM2			FM3			FM4			FM5		
	PSPC		CCD	PSPC		CCD	PSPC		CCD	PSPC		CCD	PSPC		CCD
Energy (keV)	W90	HEW	FWHM	W90	HEW	FWHM	W90	HEW	FWHM	W90	HEW	FWHM	W90	HEW	FWHM
1.5	57	15.2	8.4	57	15.1	6.6	49	13.6	6	58	12.8	4.5	55	11.1	4.3
4.5	117	15.4	8.3	139	15.8	7.3	-----	-----	-----	135	13	4.5	-----	-----	-----
6.4	169	15.2	8.2	147	15.3	6.6	-----	-----	-----	158	12.5	4.4	-----	-----	-----
8.0	161	14.4	7.7	182	14.8	6.6	153	12.5	5.1	130	12.2	4.2	211	10.9	4.7
9.9	-----	14.3	7.3	-----	-----	-----	-----	-----	-----		12.3	4.4	-----	-----	-----

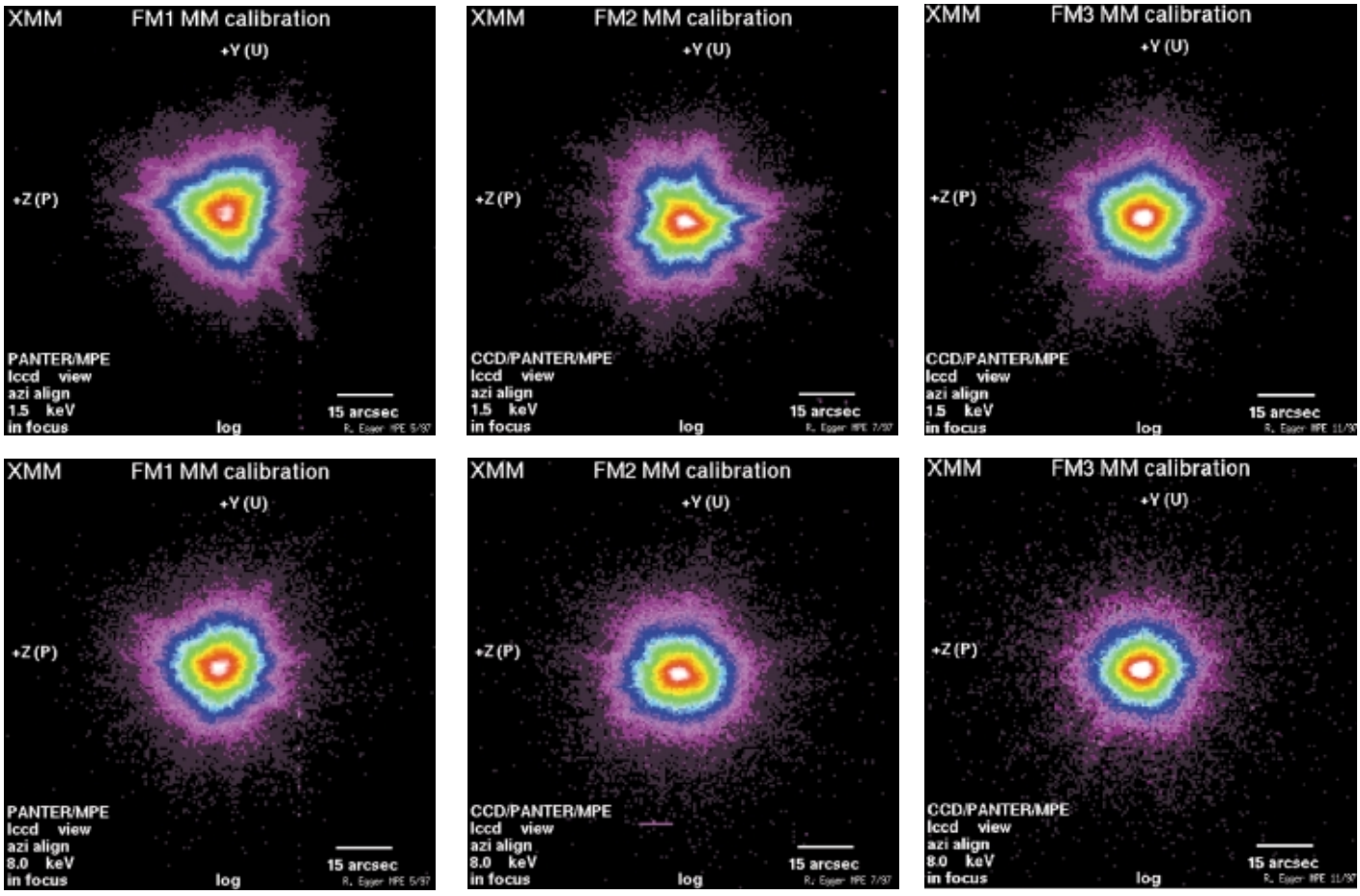

Figure 9. Close-ups of the focal image of the FM1, FM2 and FM3 Mirror Modules at 1.5 and 8 keV. (Courtesy of MPE, Neuried, Germany)

Table 4. On-axis effective area measurements (in cm^2) at 1.5 and 8.0 keV (compared to specification and theoretical measurements)

	Energy	FM1	FM2	FM3	FM4	FM5	Specification	Theory	
Full illumination	1.5 keV	911	900	932	905	906	N/A	1074	Theory
(i.e. divergent beam)	8 keV	270	275	284	284	301	N/A	341	using B.L. Henke
Reduced beam aperture	1.5 keV	not done	1430	1445	1403	On-going	1475	1560	constants
(i.e. quasi parallel beam)	8 keV	not done	618	600	593	On-going	580	686	July 93

Figure 10. Test of XMM Mirror Module with its X-ray baffle at Centre Spatial Liège (CSL), B

Table 5. X-ray baffle performance in terms of image quality, effective area and stray-light rejection

	FM2	FM3	FM4
Stray-light rejection at 60 arcmin in %	80	80	80
PSF difference for HEW/ 90W (in arcsec) before and after mounting	0/2	0.1/3	0.1/2
On-axis effective area difference (in %) before and after XRB mounting	2.2	1.1	0.2

The following tests were performed before and after the mounting of the X-ray baffle:

– effective-area measurement at various off-axis angles (between –20 arcmin and +20 arcmin) in two orthogonal directions at 58 nm
– on-axis effective area and Point Spread Function measurement at 58 nm
– X-ray pencil-beam scanning on the Mirror Module aperture to check for possible misalignment between the mirrors and the baffle.

Four Flight Models were equipped and tested with their X-ray baffles. The test results (for the three telescopes to be flown) are indicated in Table 5 and in Figures 11, 12 and 13.

In Figure 11, the evaluations of the images taken with the CCD at the EPIC detector position confirm that the intensity of the hyperboloid reflections was clearly attenuated by the presence of the baffle. Only the central part of the EPIC area is shown (EPIC diameter corresponds to the width of the image). This corresponds to a combination of 9 CCD images taken at CSL. In the left-hand image, the (shiny white) rings are due to single reflection on the hyperboloids of the outer mirrors. In the right-hand image, their intensity is strongly attenuated because of the presence of the X-ray baffle. The true (paraxial) focus is located below and outside the image. When analysing, more closely, several images at different off-axis angles, a difference between the mirrors could be observed. Reflections on the large mirrors were more blocked than on the small mirrors due to the chosen position of the sieves of the baffle. Indeed, some rays (at a small off-axis angle of about 15 - 20 arcmin) were able to pass through the sieves of the X-ray baffle and reflect directly on the

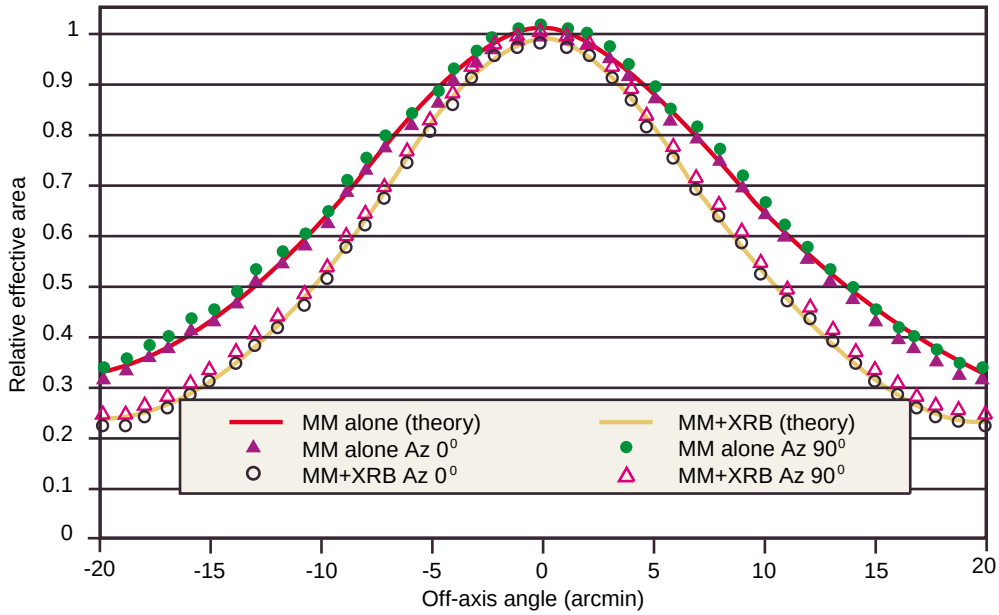

Figure 11. X-ray baffle performance in terms of image quality, effective area and stray-light rejection

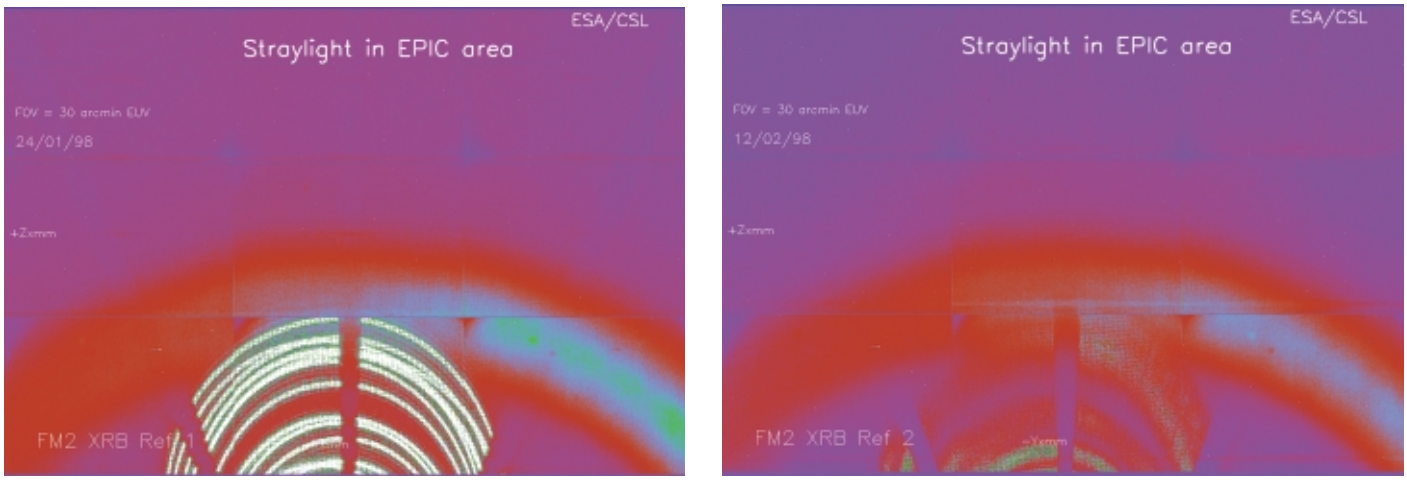

Figure 12. EPIC focal image during EUV stray-light tests on the FM2 Mirror Module without (left) and with X-ray baffle (right) for an off-axis angle of 30 arcmin

hyperboloids of these mirrors. This is because it was not possible to mount a sieve close enough to the mirrors due to the shape of the Mirror Module spider. This was clearly confirmed by the various simulations.

Table 5 shows that for the integrated X-ray baffles, there was no measurable degradation of image quality (PSF) and of the effective on-axis area. The normalised relative effective-area measurements of the Mirror Module with and without the baffle (performed in two orthogonal directions) matched the predictions with a precision better than ±2% (Fig. 11). The stray-light rejection, which is defined as the ratio of the intensity of the image of the single hyperboloid reflections before and after the mounting of the baffle was close to the prediction of 80% for all measured off-axis angles between 20 and 70 arcmin (Figs. 12 & 13).

The X-ray pencil-beam scan tests have also quantitatively confirmed that the position of the vane strips is in the 'shadow' of the mirrors. The measurements were performed with an accuracy better than 100 µm along the two scanned azimuth directions.

Conclusion and future perspective

The development of the XMM telescopes has been very successful. The continuous effort executed under the direct management of ESA to improve the quality of the mirrors and to develop the X-ray baffle has led to excellent results:

- all Flight-Model Mirror Modules have a resolution performance around 14 arcsec (HEW) at energies between 0.9 keV and 12 keV, values that are consistent with the 20 arcsec in-orbit requirement
- measurements on the Qualification-Model Mirror Module with the EPIC p-n camera, made at the Panter facility, have indicated that the Mirror Module is able to collect and sharply focus X-rays up to 17 keV (few cm^2) with a resolution (HEW) of around 15 arcsec
- the performance of the X-ray baffle is according to prediction: it rejects 80% of the stray light (coming from small-angle off-axis sources) without affecting the on-axis performance of the telescope.

The Flight-Model XMM X-ray telescopes, with their superb performance, will undoubtedly bring an important benefit to astronomers, especially for the spectroscopic part of the mission. The addition of the X-ray baffle will also considerably improve the scientific value of the XMM mission by reducing most of the X-ray and optical stray-light sources located just outside the field of view of the detectors.

The effort spent on the production of the five Flight Models of the XMM Mirror Modules (Fig. 14) and the systematic analysis of all of the mirrors produced (about 700 in total including dummies) has led to mirror shells of which the quality is largely determined by the performance of the master mandrels (i.e. HEW = 4 - 5 arcsec). Based on current knowledge, nickel-electroforming technology has been

Figure 13. Integrated collecting area (in log scale) of telescope 3 (no RGA) as a function of off-axis angle

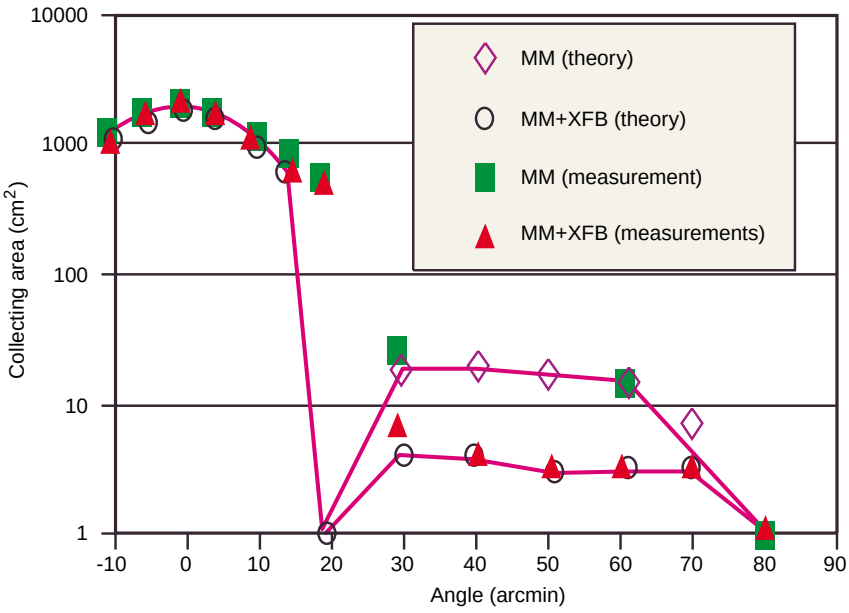

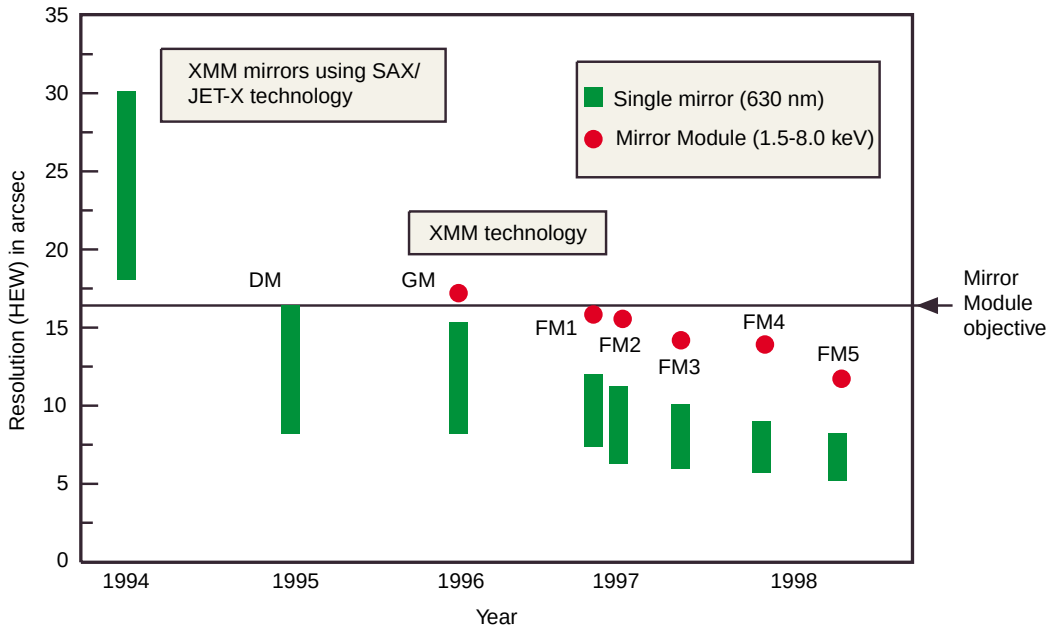

Figure 14. XMM mirror and Mirror Module performance

further improved to deliver lightweight thin mirrors with still better resolutions than those obtained for the XMM mission. Areas of investigation include the improvement of the mechanical properties of the electrolytic nickel. Some promising results have already been obtained by producing thin mirrors with a thickness of 200 µm for a diameter of 700 mm (i.e. 1/5th of the current XMM mirror thickness).

In Europe we now have a very advanced understanding of the production of thin optics using the nickel-electroforming replication technique. Such technology can, of course, be used not only for future X-ray missions (e.g. Xeus, Constellation X), but also for normal-incidence optics such as thin flexible mirrors for adaptive-optic systems, microwave high-accuracy reflectors or cavities.

Acknowledgement

The XMM mirrors were developed and manufactured by ESA and Media Lario (Bosisio Parini, Italy) with the support of:

- APCO (Vevey, Switzerland) for the manufacture of the structural parts and the containers
- BCV-Progretti (Milan, Italy) for the optical and structural analysis
- Kayser Threde (Munich, Germany) for the mechanical design and the analysis.

The optical and X-ray stray-light work was conducted by ESA and Dornier (Friedrichshafen, Germany) with the support of:

- Breault Research Organization (BRO) Inc. (Tucson, Arizona, USA) for the optical stray-light analysis
- Dornier (Ottobrunn, Germany) for the large-angle stray-light tests (including the test-setup development)
- Contraves (Zurich, Switzerland) for the design and manufacture of the entrance baffles
- Sener (Las Arenas, Spain) for the design and manufacture of the X-ray baffles.

The two Reflection Grating Assemblies (RGAs) were developed and manufactured by Columbia University, the University of California (Berkeley), Lawrence Livermore National Laboratory and Space Research Organisation Netherlands (SRON), with financing from NASA.

Our congratulations go to the industrial team for the work achieved, especially to P. Radaelli and G. Grisoni from Media Lario, Y. Gutierrez from Sener, and E. Hölzle, D. Schink and W. Rühe from Dornier. The members of the Telescope Advisory Group, Dr. B. Aschenbach and Dr. H. Bräuninger from the Max-Planck Institute in Garching, Dr. P. de Korte from Space Research Organisation Netherlands in Utrecht, and Dr. R. Willingale from the University of Leicester, as well as ESA staff are thanked for their continuous support during the mirror development effort. Our thanks also go to the testing teams at the Max-Planck Institute, at Centre Spatial de Liège and at Dornier-Ottobrunn, with special mention of R. Egger, J.P. Tock, H. Hansen, I. Domken, Y. Stockman, C. Wührer and R. Birkl. The contributions of P. Gondoin and A. Hawkyard in the early phase of the mirror development effort are also gratefully acknowledged.